
Article:
Luo, P., Yao, W., Susmel, L. orcid.org/0000-0001-7753-9176 et al. (2 more authors) (2017) A survey on multiaxial fatigue damage parameters under non-proportional loadings. Fatigue & Fracture of Engineering Materials and Structures, 40 (9). pp. 1323-1342. ISSN 8756-758X

https://doi.org/10.1111/ffe.12659

A survey on multiaxial fatigue damage parameters under non-proportional loadings

Peng Luo [1], Weixing Yao[2*], Luca Susmel[3], Yingyu Wang[1], Xiaoxiao Ma[1]

(1 Key Laboratory of Fundamental Science for National Defense-Advanced Design Technology of Flight Vehicle, Nanjing University of Aeronautics and Astronautics, Nanjing 210016, China

2 State Key Laboratory of Mechanics and Control of Mechanical Structures, Nanjing University of Aeronautics and Astronautics, Nanjing 210016, China

3 Department of Civil and Structural Engineering, the University of Sheffield, Sheffield S1 3JD, UK)

* Corresponding author. Tel.: +86 25 84892177

E-mail address: wxyao@nuaa.edu.cn

ABSTRACT

In this paper, several multiaxial fatigue damage parameters taking into account non-proportional additional hardening are reviewed. According to the way non-proportional additional hardening is considered in the model, the damage parameters are classified into two categories: (i) equivalent damage parameters and (ii) direct damage parameters. The equivalent damage parameters usually define a non-proportional coefficient to consider non-proportional additional cyclic hardening, and make a combination of this non-proportional coefficient with stress and/or strain quantities to calculate the equivalent

damage parameters. In contrast, the direct damage parameters are directly estimated from the stress and strain quantities of interest. The accuracy of four multiaxial fatigue damage parameters in predicting fatigue lifetime is checked against about 150 groups of experimental data for 10 different metallic materials under multiaxial fatigue loading. The results revealed that both Itoh's model, one of equivalent damage parameters, and Suemel's model, which belong to direct damage parameters, could provide a better correlation with the experimental results than others assessed in this paper. So, direct damage parameters are not better than the equivalent damage parameters in predicting fatigue lifetime.

Key words: multiaxial fatigue; non-proportional additional hardening; equivalent damage parameters; direct damage parameters

NOMENCLATURE

b	fatigue strength exponent
b_0	shear fatigue strength exponent
b_{-1}	bending fatigue limit under R=-1
c	fatigue ductility exponent
c_0	shear fatigue ductility exponent
C_A	half of the longest chord of the loading path
E	Young's modulus
E_r	error index

f_{-1}	axial fatigue limit under R=-1
f_{np}	coefficient quantifying additional non-proportional cyclic hardening
H	phase-difference coefficient
H_s	filling coefficient
k	material constant
K’	cyclic strain hardening coefficient
K_c	non-proportional factor for circular loading paths
l_{np}	non-proportional factor expressing the severity of non-proportional loading
m	easy glide direction
n’	cyclic strain hardening exponent
N	number of cycles to fatigue crack initiation
N_{cal}	calculated number of cycles to failure
N_{exp}	experimental number of cycles to failure
n	material constant
p, q, r	material constants
S	constant coefficient, S = 1 or S = 2
$\bar{S}_c$	statistically average value of the dislocation free movement spacing on the slip plane under the circular loading path
$\bar{S}_n$	statistically average value of the dislocation free movement spacing on the slip plane under non-proportional loading paths
$\bar{S}_p$	statistically average value of the dislocation free movement spacing on the slip plane under the proportional loading path
T	cycle period

t_{-1}	torsional fatigue limit under R=-1
t_k	time instant
T_Σ	maximum value of macroscopic shear stress
$W(t_k)$	weight function
α_{np}	material non-proportionality factor
γ_{eq}	equivalent shear strain
γ_f'	shear fatigue ductility coefficient
γ_{max}	maximum shear strain
$\Delta\gamma_{\Delta 45}$	shear strain range at $\alpha = 45^\circ$ to maximum shear plane
$\Delta\gamma_{max}$	maximum shear strain range
$\Delta\gamma^p_{max}$	maximum plastic shear strain range
ε_f'	fatigue ductility coefficient
$\varepsilon_1(t)$	maximum absolute value of principal strains at time t, $\varepsilon_{1max} = \max[\varepsilon_1(t)]$
$\Delta\varepsilon_1$	maximum principal strain range
$\Delta\varepsilon_n$	normal strain range
θ	angle of the cycle path orientation with respect to the principal axis
λ	strain ratio, $\lambda = \gamma_a / \varepsilon_a$
ν	Poisson's ratio
$\xi(t)$	angle between ε_{1max} and $\varepsilon_1(t)$
ρ	stress ratio of the crack initiation plane and $\rho = \sigma_n^{max}(\phi^*, \theta^*) / \tau_a(\phi^*, \theta^*)$
σ_a	normal stress amplitude

σ_b	tensile strength
σ_{eq}	equivalent stress
σ_f'	fatigue stress coefficient
σ_n^{max}	maximum normal stress during a loading cycle
σ_y	yield strength
$\Delta\sigma_n$	normal stress range
τ_{-1}	modified shear fatigue limit
τ_a	shear stress amplitude
τ_f'	shear fatigue stress coefficient
$\tau_{\alpha_{CPA}}^{MDP}$	equivalent shear stress on the critical plane determined according to McDiarmid
ϕ	phase angle of non-proportional loadings
$\phi(t_k)$	maximum principal stress direction at time t_k
ϕ	weighted mean principal stress direction
$\mu\gamma_{pl,i}$	microscopic plastic shear strain amplitude in the i-th cycle
Γ	cumulated plastic strain

1 Introduction

Mechanical components usually undergo multiaxial fatigue loadings, which could be non-proportional and random. It is important for structural engineers to accurately estimate fatigue strength of metallic materials under multiaxial fatigue loadings to avoid unwanted

in-service failures. The problem of designing real components and structures against multiaxial fatigue is very complex due to the effect of additional non-proportional cyclic hardening under multiaxial non-proportional loadings. The effect of additional non-proportional cyclic hardening on multiaxial fatigue damage must be considered properly in modelling the crack initiation process, in estimating the cumulated fatigue damage as well as in predicting fatigue lifetime. Many fatigue damage parameters have been proposed by researchers over the years, such as the parameters devised by Brown and Miller [1], Papadopoulos [2], Sines [3], Findley [4] and many more. In general, Multiaxial fatigue damage parameters are subdivided into the following three different groups [5-7]: equivalent stress/strain criteria, critical-plane criteria and energy criteria. The equivalent stress/strain criteria (that are based on static strength approaches) give satisfactory estimates of multiaxial fatigue lives under in-phase fatigue loadings. However, these criteria are not suitable for predicting fatigue lifetime under multiaxial out-of-phase fatigue loading. Critical-plane criteria take into account not only the magnitude of stresses and strains, but also the orientation of the associated crack initiation plane. Energy criteria are able to describe the fatigue problem and, under particular circumstances, give a relatively better prediction of fatigue lives under multiaxial loading. However, the main problem associated with the use of

these criteria is that energy is a scalar quantity and it is not suitable for estimating the orientation of those planes on which fatigue cracks initiate and propagate. In order to overcome this limitation, several critical plane-strain energy density criteria have been proposed and validated [8-10], with these approaches being based on a combination of the energy criteria and the critical plane concept in order to improve the accuracy in predicting fatigue lifetime.

According to the way additional non-proportional cyclic hardening is usually assessed, this paper classifies multiaxial fatigue damage parameters into two categories: (i) equivalent damage parameters and (ii) direct damage parameters. The fundamental difference between these two types of parameter is whether a non-proportional coefficient is used to calculate the multiaxial damage parameter of interest. Equivalent damage parameters perform qualitative analyses to assess the effect of non-proportional loadings, and make a combination of non-proportional coefficients and stress and/or strain quantities to predict fatigue life. However, additional non-proportional cyclic hardening effect is directly taken into account through stress and/or strain quantities in direct damage parameters.

In this paper, some popular multiaxial fatigue damage parameters proposed in recent years are reviewed. Among them, four typical models are evaluated based on almost 150

groups of experimental data in order to find out the most reliable engineering solutions for different materials.

2 Equivalent damage parameters

The equivalent damage parameters are developed by introducing the coefficient of non-proportionality, which is designed to quantify the severity of the degree of non-proportionality of the load history being assessed. To be convenient to compare the following parameters with each other, the adopted symbols are unified as follows:

l_{np} is a non-proportional factor quantifying the severity of non-proportional load histories;

α_{np} is a material parameter quantifying the non-proportional factor characterizing the material under investigation;

f_{np} is the coefficient of the non-proportional additional cyclic hardening;

ϕ is the out-of-phase angle characterizing the non-proportional loading.

Generally speaking, the correlation between $f_{np,}$ l_{np} and α_{np} can be expressed as follows:

$$f_{np} = f(\alpha_{np}, l_{np}) \tag{1}$$

where f is a function that varies with the characteristics of damage parameter being used.

Kanazawa, Miller and Brown et al. [11-12] investigated the low-cycle fatigue strength

problem and the stabilized cyclic stress-strain response of l% Cr-Mo-V steel under out-of-phase combined axial and torsional loadings. Their experimental results clearly suggest that the plane of slip bands is much closely aligned with the material plane experiencing the maximum shear stress amplitude. Garud [12] has a similar point of view. Kanazawa et al. [11] defined a principal axes rotation factor, in terms of the amount of slips experienced by the critical planes in the specimen. The rotation factor is defined as the ratio of the shear strain range on the maximum shear strain plane and that on the plane having 45° included angle to the maximum shear strain plane. Then the loadings non-proportional factor is defined as follows [11]:

$$\mathrm{l}_{\mathrm{np}}=\frac{\Delta\gamma_{\Delta 45}}{\Delta\gamma_{\max}}=\left(\frac{\lambda^2+(1+\nu)^2-\sqrt{\left((1+\nu)^2-\lambda^2\right)^2+\left(2\lambda(1+\nu)\cos\phi\right)^2}}{\lambda^2+(1+\nu)^2+\sqrt{\left((1+\nu)^2-\lambda^2\right)^2+\left(2\lambda(1+\nu)\cos\phi\right)^2}}\right)^{1/2} \tag{2}$$

The equivalent shear strain is

$$\gamma_{\mathrm{eq}}=\mathrm{k}\cdot\gamma_{\max}\cdot\mathrm{f}_{\mathrm{np}}=\mathrm{k}\cdot\gamma_{\max}\cdot(1+\alpha_{\mathrm{np}}\cdot\mathrm{l}_{\mathrm{np}}) \tag{3}$$

where $\mathrm{k}=\mathrm{f}_{-1}/\mathrm{t}_{-1}$ is the ratio of fully reversed axial fatigue limit and torsional fatigue limit.

Through observations and analyses of the experimental results of 1045 HR steel and Inconel 718 under biaxial fatigue loading, Fatemi [14][14] proposed to replace the normal strain term on the maximum shear plane in Brown and Miller's equation with a normal stress on that plane, so that the additional cyclic hardening of materials due to the rotation of the principal

axes during non-proportional loadings can be accounted for. The non-proportional loading factor is defined as follows:

$$l_{np} = \frac{\sigma_n^{max}}{\sigma_y} \tag{4}$$

where σ_y and σ_n^{max} are the yield strength and the maximum normal stress during the loading cycle, respectively.

The equivalent shear strain is defined as

$$\gamma_{eq} = \frac{\gamma_{max}}{2} f_{np} = \frac{\gamma_{max}}{2}\left(1+\alpha_{np} l_{np}\right) \tag{5}$$

Lee [15] proposed a parameter based on Gough's elliptic equation. However, this solution is restricted to particular loading cases. The form of the parameter is:

$$f_{np} = 2\left(1+\alpha_{np}\sin\phi\right) \tag{6}$$

For proportional loadings, f_{np}=2, the damage parameter coincides with Gough's elliptic equation. For non-proportional loadings, the equivalent damage parameter can be written as:

$$\sigma_{eq} = \sigma_a\left[1+\left(\frac{b_{-1}}{2t_{-1}}\frac{2\tau_a}{\sigma_a}\right)^{f_{np}}\right]^{1/f_{np}} \tag{7}$$

where σ_a is the amplitude of normal stress, τ_a is the amplitude of shear stress, b_{-1} and t_{-1} are the bending fatigue limit under R=-1 and the torsional fatigue limit under R=-1 respectively.

Itoh et al. [16] carried out a series of constant amplitude low-cycle fatigue tests under different multiaxial cyclic strain paths and found that non-proportional low-cycle fatigue

strength is significantly influenced by the changed range of the principal strain direction and the strain paths. The non-proportional factor that expresses the severity of the non-proportional loading under investigation is defined as follows:

$$l_{np} = \frac{1.57}{T\varepsilon_{1max}} \int_0^T |\sin \xi(t)| \varepsilon_1(t) dt \tag{8}$$

where $\varepsilon_1(t)$ is the maximum absolute value of the principal strains at instant t, $\varepsilon_{1max} = \max[\varepsilon_1(t)]$, $\xi(t)$ is the angle between ε_{1max} and $\varepsilon_1(t)$, T is loading period, respectively.

Based on previous studies by Itoh [16], Itoh and Yang [17] further found that the reduction of fatigue life in the low-cycle fatigue regime due to non-proportional loading is related to the effect of the additional cyclic hardening. Then they developed a suitable expression of the material constant which is closely related to the static deformation behavior of the material. The formulation of the material constant can be expressed as:

$$\alpha_{np} = S \frac{\sigma_b - \sigma_y}{\sigma_b} \tag{9}$$

where σ_b is tensile strength, σ_y is yielding stress or 0.2% proof stress, coefficient S takes S=1 for face-centered cubic structure (FCC) materials and S=2 for body-centered cubic structure (BCC) materials.

Choosing the maximum principal strain range as the equivalent damage parameter, the fatigue damage parameter of Itoh model can be written as follows:

$$\varepsilon_{eq} = \Delta\varepsilon_I \, f_{np} = \Delta\varepsilon_I (1 + \alpha_{np} \, f_{np}) \tag{10}$$

where $\Delta\varepsilon_I$ is the maximum principal strain range with $\Delta\varepsilon_I = \max[\varepsilon_{Imax} - \cos\xi(t) \cdot \varepsilon_I(t)]$.

Many other researchers, such as Chen [18] and Durprat [19] have developed their own approaches on the basis of Itoh's method.

Borodii [20-22] considered the additional hardening effect resulting from the strain range and the shape of cycle loading path. In order to take the influence of the strain paths into account, a number of parameters (stress/strain/energy) have been proposed to establish an unambiguous relation between loading path and strain hardening. Then Itoh's strain criterion[16] was modified. The relative change between the cycle path direction and the principal strain axis is taken into account by Borodii [22] in the new coefficient of non-proportionality. The modified non-proportionality of multiaxial loadings and the new coefficient of non-proportionality are defined as follows:

$$l_{np} = \left(\left| \oint_{L'} \bar{e} \times d\bar{e} \right| / \left| \oint_{L_0} \bar{e} \times d\bar{e} \right| \right)^r \tag{11}$$

$$f_{np} = (1 + k \sin\theta)(1 + \alpha_{np} l_{np}) \tag{12}$$

where $\bar{e}$, $d\bar{e}$ are the vectors of strain and strain increment respectively; L' is the deformation path of the cycle or the convex equivalent path of the cycle; L_0 is the circular path; the procedure of determination of the exponent r is contained in Appendix A of

reference [21]; k is the material constant which characterizes the difference in the cyclic properties (from the lifetime) for proportional strain paths and is commonly obtained by experiments; θ is the angle of the cycle path orientation with respect to the principal axis. The equivalent damage parameter is expressed as follows:

$$\varepsilon_{eq} = f_{np}\Delta\varepsilon_1 \tag{13}$$

He et al. [23] investigated the microscopic mechanism of the decrease of materials' fatigue lifetime under non-proportional loadings, and found that more micro cracks initiate under low-cycle fatigue complex non-proportional loading than those initiate under proportional loadings. The increasing number of micro cracks accelerates the propagating rate of the subsequent fatigue cracks. The non-proportional factor of the strain path is defined as the distribution of the dislocation free movement spacing on the slip plane which can be expressed as follows:

$$l_{np} = K_c \frac{\left(\bar{S}_n / \bar{S}_p\right)^{-1/2} - 1}{\left(\bar{S}_c / \bar{S}_p\right)^{-1/2} - 1} \tag{14}$$

where $\bar{S}$ is the statistically average value of the free movement spacing of the dislocations on the slip plane under the loading of identical equivalent strain amplitudes but different loading paths. In Eq. (14), subscripts n, c and p denote non-proportional loadings path, circular loadings path and proportional loadings path, respectively. K_c is the non-proportional

factor of the circular loadings path.

If the maximum amplitude of the shear strain on the critical plane is selected as the equivalent damage parameter for the life prediction, the equivalent shear strain can be written as:

$$\gamma_{eq} = k \cdot \frac{\Delta\gamma^{p}_{max}}{2} \cdot \left(1+\alpha_{np} l_{np}\right)^{1/n} \tag{15}$$

where k is a material constant. Therefore, the coefficient of non-proportionality takes on the following form [23]:

$$f_{np} = (1+\alpha_{np} l_{np})^{1/n} \tag{16}$$

Li Jing et al. [24] analyzed Wang-Brown's model [25] and proposed a new effective cyclic parameter without empirical constants based on the critical plane approach. The new effective cyclic parameter contains a new stress-correlated factor to account for the additional cyclic hardening caused by non-proportional loadings. The new stress-correlated factor and effective cyclic parameter are defined as follows, respectively:

$$f_{np} = 1+\frac{\Delta\sigma_n}{2\sigma_{0.2}} \tag{17}$$

$$\varepsilon_{eq} = \frac{\Delta\gamma_{max}}{2} + f_{np}\frac{\Delta\varepsilon_n}{2} \tag{18}$$

where $\Delta\sigma_n$ is the range of normal stress and $\sigma_{0.2}$ is 0.2% proof stress.

Most of the methods mentioned above take the maximum shear plane as the critical plane, but the selected parameters describing fatigue damage are different from each other.

Further, the definitions of non-proportionality and the coefficients of the non-proportional additional cyclic hardening also differ from one another. The summary of aforementioned equivalent damage parameters is listed in Fig.1.

3 Direct damage parameters

The direct damage parameters are used to directly predict fatigue lifetime or to calculate the fatigue strength by analyzing stress components or strain components in the fatigue failure zone.

Morel [26] presented a fatigue life prediction method based on the theory of elastic homogeneous state in the mesoscopic scale. In the interpretation of this method, the initiation process of a crack is treated as a mesoscopic phenomenon occurring on a scale of the order of a grain or a few grains, and some plastically less resistant grains (mesoscopic scale) make the material fail. The phase-difference coefficient H facilitating the description of the out-of-phase mechanism is introduced to the consideration of the significant influence on the fatigue damage accumulation due to the out-of-phase loadings. H is expressed as

$$H = \frac{T_{\Sigma}}{C_A} \tag{19}$$

where T_{Σ} and C_A are the maximum value of the macroscopic shear stress and half of the longest chord of the loadings path described by the shear stress vector on the critical plane,

respectively, with these quantities being calculated via the algorithm proposed by Papadopoulos [27].

The chosen fatigue damage variable is the accumulated plastic strain at the mesoscopic scale and the number of cycles of fatigue crack initiation is

$$N = p\ln\left(\frac{C_A}{C_A - \tau_{-1}}\right) + q\frac{\tau_{-1}}{C_A - \tau_{-1}} - \frac{r}{C_A} \tag{20}$$

where p, q, r are material constants that depend on the hardening parameters, whereas $\tau_{-1} = \frac{T_{\Sigma lim}}{H} = \frac{C_A \cdot T_{\Sigma lim}}{T_\Sigma}$ is the modified shear fatigue limit.

Spagnoli & Carpinteri [28] took as a starting point the idea that there is a deviation angle between the critical plane of materials under non-proportional loadings and that under proportional loadings. In particular, a correlation between the weighted mean direction of the maximum principal stress (normal to the fatigue fracture plane) and the normal to the critical plane is proposed to modify the orientation of the critical plane. The fatigue damage parameter is defined as a nonlinear combination of the maximum normal stress N_{max} and the shear stress amplitude acting on the critical plane C_a:

$$\sigma_{eq} = \sqrt{\left(\frac{\sigma_{af}}{\tau_{af}}\right)^2 C_a^2 + N_{max}^2} \tag{21}$$

where σ_{af} and τ_{af} are the fatigue limit stress respectively deduced from the S–N curve for uniaxial tension-compression and torsion with loading ratio R=-1. The weighted mean

principal stress directions [29] are reported below:

$$\hat{\phi} = \frac{1}{W}\sum_{t_1}^{t_N} \phi(t_k) \cdot W(t_k) \tag{22}$$

where $\phi(t_k)$ is the maximum principal stress direction at time t_k, $W(t_k)$ is a weight function taking into account the main factors that influence the fatigue fracture behavior. The authors presented a weight function based on axial S-N curve as follows:

$$W(t_k) = \begin{cases} 0 & \text{if } \sigma_1(t_k) < c\sigma_{af} \\ \left(\dfrac{\sigma_1(t_k)}{c\sigma_{af}} \right)^{m_\sigma} & \text{if } \sigma_1(t_k) \geq c\sigma_{af} \end{cases} \qquad 0<c\leq 1 \tag{23}$$

where m_σ is the negative reciprocal of the slope of the S–N curve being considered. Constant c physically represents a safety factor, since it makes the considered S–N curve lower than that with the fatigue limit σ_{af}.

Susmel [30] proposed a method for estimating multiaxial high-cycle fatigue strength based on the theory of cyclic deformation in single crystals which interprets the physical mechanism of the fatigue damage. Such theory is also used to single out those stress components which can be considered significant for crack nucleation and growth in the so-called Stage I regime. The theory mentioned above employs the cumulated plastic strain Γ to weigh the fatigue damage of the single crystal. In particular, Γ is defined as follows:

$$\Gamma = \sum_{t=1}^{N} \left| \mu\gamma_{pl,i} \cdot m \right| \tag{24}$$

where $\mu\gamma_{\mathrm{pl,i}}$ is the microscopic plastic shear strain amplitude in the i-th cycle and N is the total number of cycles, m is the slip direction.

Under the hypothesis of a purely elastic macroscopic strain, the relation between the macroscopic shear stress versus the microscopic plastic shear stress can be expressed as follows[29]:

$$\tau \cdot \mathrm{m} = \mathrm{b}\left(\mu\gamma_{\mathrm{p}} \cdot \mathrm{m}\right) \tag{25}$$

where b is a monotonic function and τ is the macroscopic shear stress.

On the basis of previous research work [31-33], it is deduced that the plane experiencing maximum macroscopic shear stress amplitude can be considered coincident with the fatigue micro crack initiation plane, and the influence of the stress normal to the crack initiation plane during crack growth can be explained by transferring Socie's fatigue damage model [34-35] to the microscopic scale. The equivalent shear stress used to estimate the fatigue life can be written as:

$$\tau_{\mathrm{eq}} = \tau_{\mathrm{a}} + \left(\mathrm{t}_{-1} - \frac{\mathrm{f}_{-1}}{2}\right)\rho \tag{26}$$

where ρ is the stress ratio of the crack initiation plane which is used to take into account the influence of non-proportional loadings. $\rho = \frac{\sigma_{\mathrm{n}}^{\max}}{\tau_{\mathrm{a}}}(\phi^*, \theta^*)$ is a function of phase angle. ϕ^*, θ^* are the angles of the critical plane in spherical coordinate which is the plane experiencing

maximum shear stress amplitude.

Skibicki [36] suggested a loading non-proportionality measure based on McDiarmid's critical plane fatigue criterion [37] for the case of multiaxial fatigue. The presented loading non-proportionality parameter known as the filling coefficient, H_s, was based on observations of stress hodographs of the maximum shear stress for different loading with non-proportionality degrees. Filling coefficient H_s is defined as a quotient of the area within the hodograph and the area of the circle described on the hodograph.

$$H_s = \frac{\int_{\alpha}\left(\tau_{\alpha}^{MDP}\cdot W\right)}{\pi\left(\tau_{\alpha_{CPA}}^{MDP}\right)^2/2} \tag{27}$$

where τ_{α}^{MDP} is the equivalent stress on the material plane, α is calculated according to McDiarmid [37] relation under out-of-phase loadings, $\tau_{\alpha_{CPA}}^{MDP}$ is the equivalent stress on critical plane, $W=\sin[2(\alpha-\alpha_{CPA})]^k$ is a weight function and the index k which influences the character of changeability of the function W is obtained by experimental data fitting.

The general form of the fatigue damage parameter under non-proportional loadings was postulated by the author as follows:

$$\tau_{eq} = \tau_{\alpha_{CPA}}^{MDP}\left(1+\frac{t_{-1}}{b_{-1}}H^n\right) \tag{28}$$

where n is obtained by experimental data fitting.

In addition, Liu et al. [38] also proposed a multiaxial fatigue criterion involving the

critical plane rotation approach in which the critical plane is directly correlated with the fatigue fracture plane. Farahani [39] took the influencing factors of axial mean stress and additional hardening under out-of-phase strain path into consideration. Many other researchers such as Chu [40], Huyen [41] et al. proposed their own damage parameters correlated with the critical plane approaches and energy based approaches. Fig.2 is a summary of direct damage parameters.

4 Evaluation of multiaxial fatigue failure criteria

4.1 How to select the fatigue criteria to estimate fatigue life under multiaxial loading?

In this section, four typical multiaxial fatigue failure criteria are chosen for validation by experimental data. There are many reasons for choosing these among others fatigue failure criteria. Firstly, these four criteria have a significant influence on the other multiaxial fatigue failure criteria and are widely referenced by other researchers. Many multiaxial fatigue life prediction methods are derived from them.

Secondly, these four criteria could be used to estimate multiaxial fatigue life conveniently and do not have unambiguous definitions and contain less or no material property parameters. For example, the damage parameters proposed by Susmel[29] and Spagnoli[28] require only material constants of axial fatigue and torsional fatigue property.

Similarly, Kanazawa's [11-12] and Itoh's [16] approaches just need one extra material non-proportional parameter and in particular, the way to determine these parameters experimentally was introduced in detail in the references.

The aim for researchers is to decrease the dependence on large numbers of experiments, experiential elements and material constants as far as possible in fatigue life analyses. In consequence, the number of material property parameters can be taken as one of the standards to judge the relevance of a multiaxial fatigue criterion.

4.2 Test data collection

To avoid the inaccuracy of fatigue life prediction for a single specimen, group test data should be chosen to verify the criteria. In this paper, nearly 150 groups of multiaxial fatigue experimental data generated by testing 10 different materials under different load conditions are collected. The data about the mechanical and fatigue properties of the materials being considered are listed in Fig. 3 and Fig. 4, respectively. All the test results are under constant amplitude sinusoidal load with R=-1, and they are summarized in Fig. 5. By implementing the assessed fatigue damage parameters in specific numerical codes, their accuracy and reliability will be checked against the experimental results listed in Fig. 5.

4.3 Evaluation results and discussion

In order to measure the deviation and correlation between predicted lives and experimental lives, error index E_r is defined as shown in Fig.6.

Obviously, the closer the error index E_r is to 1, the more accurate the prediction by using multiaxial fatigue failure criterion is. The percentages of estimations obtained by using the selected four criteria that fall within different error index E_r are listed in Fig. 7. The corresponding histograms are reported in Figs. 2-5. Moreover, Fig. 7 reports the mean value and variance of error index E_r for the different fatigue critera.

According to Fig. 7, Fig. 8 and Figs. 9-12, we can find the optimum multiaxial fatigue failure criteria for these materials, see Fig. 13. The ratio between the pure torsion and tension fatigue strengths, t_{-1} / f_{-1}, is also listed in Fig. 13 to reveal the ductility of material. In general, ductile materials have ratios close to 0.5 or 0.58, whereas brittle materials have ratios approaching 1. [52]

It can be concluded from Fig. 9 to Fig. 12 that:

For all of the four methods studied above, life prediction results for different materials vary greatly. For example, predictions of 1045 stainless steel, 1Cr–18Ni–9Ti steel(75% and 93% data points respectively) can perfectly fit Kanazawa's model within a factor of 4. But the predictive capabilities of Kanazawa's model are rather poor for other chosen materials. This

indicates the fact that dispersion of fatigue life estimation is significant and the applicability of each method is limited.

Spagnoli's parameter returned very good life estimates for SM45C (86% data points respectively within a factor of 2), and reasonably good life estimates for SM45C and LY12CZ (86% and 87% data points respectively within a factor of 4).

Susmel's parameter and the Itoh's parameter returned reliable estimates for most of the collected materials, including brittle materials and ductile materials. For Susmel's parameter and Itoh's parameter, there are 9 and 8 of the 10 kinds of collected materials respectively which achieved more than 50% data points within a factor of 4.

From Figs. 9 to 12 and Fig. 5, it can be concluded that:

On the whole, it is observed that the predicted fatigue life of Susmel's and Itoh's models is close to the experimental life for designed specimens (70% and 75% of all the data points respectively within a factor of 4 in Figs.4.). But for the Kanazawa's and Spagnoli's models, only 38% and 49% of all the data points are located within a factor of 4 respectively. In other word, Suemel's and Itoh's models are more accurate and stable than others.

The direct damage parameters are generally derived through rigorous theoretical deduction without empirical and experimental elements while the equivalent damage

parameters depend more on the experimental data and material coefficients. However, the life estimation results prove that direct damage parameters are not better than the equivalent damage parameters due to the fact both Suemel's and Itoh's models could provide a good correlation with the experimental results.

Each method includes more or less empirical and experimental constants and the life prediction result of each method for different materials is unstable, so far there isn't a multiaxial fatigue theory which is universally applicable.

5.Conclusions

(1) The non-proportional equivalent damage parameters are mostly developed from proportional multiaxial fatigue damage parameters which are relatively mature and widely proved. They can be understood intuitively, deduced concisely and employed conveniently and easily, but sometimes they could lead to large errors because of their great dependence on the empirical and experimental components.

(2) The direct damage parameters are generally derived through rigorous theoretical deduction, but most of them use classical and ideal theories of single crystal theory, elastic homogeneous state and elastic-plastic damage accumulation theory and so on. The methods using direct damage parameters to predict fatigue life are restricted to simple working

conditions of engineering structures due to their ideal assumptions which are different from the actual situations.

(3) The research in the future is to establish a widely applicable multiaxial fatigue failure criterion in engineering. At present, there are several important problems needed to be solved such as how to consider the impact of the mean value and loadings path of non-proportional loadings on high and low cycle fatigue life, and meanwhile how to reduce the material constants and simplify the uncertain parameters in the criteria.

References

[1] Brown, M.W. and Miller, K.J. (1982) Two decades of progress in the assessment of multiaxial low-cycle fatigue life. In: Amzallag C, Leis B, Rabbe P, editors. Low-cycle fatigue and life prediction, ASTM STP 770. 482–99.

[2] Papadopoulos, I.V., Davoli, P., Gorla, C., Fillippini, M.and Bernasconi, A. (1997) A comparative study of multiaxial high-cycle fatigue criteria for metals. Int. J. of Fatigue ,**19**,219-35.

[3] Sines, G. (1959) Behaviour of metals under complex stresses. Metal Fatigue. 145–69.

[4] Findley, W.N. (1959) A theory for the effect of mean stress on fatigue of metals under combined torsion and axial load or bending. J. Eng. Ind. Trans. ASME,**81**,301–6.

[5] Zhu, Z.Y., He, G.Q., Zhang, W.H. and Liu, X.S.(2006) Recent advances on microscopic mechanism of multiaxial fatigue under non-proportional loading. J. of TongJi University, **34**, 1510-1514.

[6] Feng, C.Y. (2010) Recent development of study on multiaxial low cycle fatigue under non-proportional loadings. Corrosion Science and Protection Technology, **22**, 124-127.

[7] Liu, L.L. and Nie, H. (2009) General description of multiaxial low cycle fatigue under non-proportional loading. J. of North China Institute of Sci. and Tech., **6**, 60-63.

[8] Chu, C.C., Conle, F.A. and Bonnen, J.J. (1993) Multiaxial stress-strain modeling and fatigue life prediction of SAE axle shafts. In: Edited by McDowell DL, Ellis R. Advances in Multiaxial Fatigue, ASTM STP 1191, 37-54.

[9] Glinka, G., Plumtree, A. and Shen G. A. (1995) Multiaxial fatigue strain energy parameter related to the critical plane. Fatigue Fract Eng. Mater. Struct., **18**, 37-46.

[10] Glinka, G., Wang G. and Plumtree, A. (1995) Mean stress effects in multiaxial fatigue. Fatigue Fract. Eng. Mater. Struct., **18**, 755-764.

[11] Kanazawa, K., Miller, K.J., and Brown, M.W. (1979) Cyclic deformation of 1% Cr-Mo-V steel under out-of-phase loads. Fatigue Fract. Eng. Mater. Struct., **2**, 217-228.

[12] Kanazawa, K., Miller, K. J., and Brown, M. W. (1977). Low-cycle fatigue under

out-of-phase loading conditions. J. of Eng. Mat. Tech., **99**, 222.

[13] Garud, Y.S. (1981) A new approach to the evaluation of fatigue under multiaxial loadings. J. of Eng. Mater. and Tech., **103**, 118-126.

[14] Fatemi, A. and Socie, D. F. (1988) A critical plane approach to multiaxial fatigue damage including out-of-phase loading. Fatigue Fract. Eng. Mater. Struct., **11**, 149-165.

[15] Lee, S.B. (1989) Out-of-phase combined bending and torsion fatigue of steels. Biaxial and Multiaxial Fatigue, EGF 3, Mechanical Engineering Publications, 621~634.

[16] Itoh, T., Sakane, M., Ohnami, M. and Socie, D.F. (1995) Non-proportional low cycle fatigue criterion for type 304 stainless steel. Int. J. of Fatigue, **117**,285-292.

[17] Itoh, T., and Yang, T. (2011) Material dependence of multiaxial low cycle fatigue lives under non-proportional loading. Int. J. of Fatigue ,**33**,1025-1031.

[18] Chen, X. (1996) Low-cycle fatigue under non-proportional loading. Fatigue Fract. Eng. Mater. Struct. , **19**, 837-854.

[19] Duprat, D. (2013) A model to predict fatigue life of aeronautical structures with out-of-phase multiaxial stress condition. Proc. Fifth International Conference on Biaxial/multiaxial Fatigue and Fracture, Technical University of Opole, **1**, 111-123.

[20] Borodii, M.V. (1996) Engineering method of determining non-proportionality parameter

under biaxial fatigue loading. ASME Pressure Vessels & Piping Conf. Montreal, **323**,21-26.

[21] Borodii, M.V.and Strizhalo, V.A. (2000) Analysis of the experimental data on a low cycle fatigue under non-proportional straining. Int. J. of Fatigue, **22**, 275-282.

[22] Borodii, M.V. and Adamchuk, M.P. (2009) Life assessment for metallic materials with the use of the strain criterion for low cycle fatigue. Int. J. of Fatigue, **31**, 1579-1587.

[23] He, G. Q., Chen, C. S., Ding, X. Q., and Xu, R. X. (2004). New low cycle fatigue life criterion under nonproportional loading based on critical plane methods. J. of Tongji University, **32**, 1637-1641.

[24] Li, J. (2010). The biaxial fatigue life prediction model based on the critical plane approach under combined loading of tension and torion. Chinese J. of Solid Mech., **31**, 101-106.

[25] Wang, C.H. and Brown, M.W. (1993) A path-independent parameter for fatigue under proportional and non-proportional loading. Fatigue Fract. Eng. Mater. Struct., **16**, 1285-1298.

[26] Morel, F. (1998) A fatigue life prediction method based on a mesoscopic approach in constant amplitude multiaxial loading. Fatigue Fract. Eng. Mater. Struct.,**21**, 241-256.

[27] Papadopoulos, I.V., Davoli, P., Gorla, C., Filippini, M., and Bernasconi, A. (1997). A comparative study of multiaxial high-cycle fatigue criteria for metals. Int. J. of Fatigue, **19**, 219-235.

[28] Spagnoli, A. (2001) A new high-cycle fatigue criterion applied to out-of-phase biaxial state. Int. J. of Mech. Sci., 43, 2581-2595.

[29] Carpinteri, A., Macha, E., Brighenti, R., and Spagnoli, A. (1999). Expected principal stress directions under multiaxial random loading. part I: theoretical aspects of the weight function method. Int. J. of Fatigue, **21**, 83-88.

[30] Susmel, L., and Lazzarin, P. (2002) A bi-parametric Wohler curve for high cycle multiaxial fatigue assessment. Fatigue Fract. Eng. Mater. Struct., **25**, 63-78.

[31] Lazzarin, P., and Susmel, L. (2003) A stress-based method to predict lifetime under multiaxial fatigue loadings. Fatigue Fract. Eng. Mater. Struct., **26**,1171-1187.

[32] Susmel, L., Tovo, R., and Lazzarin, P. (2005) The mean stress effect on the high-cycle fatigue strength from a multiaxial fatigue point of view. Int. J. of Fatigue, **27**,928-943.

[33] Susmel, L. (2008) Multiaxial fatigue limits and material sensitivity to non-zero mean stresses normal to the critical planes. Fatigue Fract. Eng. Mater. Struct., **31**,295-309.

[34] Socie, D. F., Waill, L. A. and Dittmer, D. F. (1985) Biaxial fatigue of Inconel 718

including mean stress effects. In: Multiaxial Fatigue, ASTM STP 853, American Society for Testing and Materials,463-481.

[35] Socie, D. F. (1987) Multiaxial fatigue damage models. Trans. ASME J. Eng. Mater. Technol. **109**, 293-298.

[36] Skibiciki, D., and Sempruch, J. (2004) Use of a load non-proportionality measure in fatigue under out-of-phase combined bending and torsion. Fatigue Fract. Eng. Mater. Struct., **27**, 369-377.

[37] McDiarmid, D.L. (1991) A general criterion for high cycle multiaxial fatigue failure. Fatigue Fract. Eng. Mater. Struct. **14**, 429-453.

[38] Liu, Y., and Mahadevan, S. (2005) Multiaxial high-cycle fatigue criterion and life prediction for metals. Int. J. of Fatigue, **27**, 790-800.

[39] Farahani, A.V. (2000) A new energy critical plane parameter for fatigue life assessment of various materials subjected to in-phase and out-phase multiaxial fatigue loading conditions. Int. J. of Fatigue, **22**, 295-305.

[40] Chu, C. C. (1995). Fatigue damage calculation using the critical plane approach. J. of Eng. Mat. Tech., **117**,41-50.

[41] Huyen, N., Flaceliere, L., and Morel, F. (2008) A critical plane fatigue model with

coupled meso-plasticity and damage. Fatigue Fract. Eng. Mater. Struct., **31**, 12-28.

[42] Kallmeyer, A.R., Krgo, A., and Kurath, (1989) P. Evaluation of multiaxial fatigue life prediction methodologies for Ti-6Al-4V. Diss. Abstr. Int.,**50**,178.

[43] Zhang, C.C. (2010) Fatigue life prediction of structures in HCF region under complex stress field, Nanjing University of Aeronautics and Astronautics Ph.D. Thesis,11-17.

[44] Nishihara, T., and Kawamoto, M. (1941). The strength of metals under combined alternating bending and torsion. J. of the Japan Society of Mech. Eng., **44**, 722-723.

[45] Doong, S. H., Socie, D. F., and Robertson, I. M. (1990). Dislocation substructures and non-proportional hardening. J. of Eng. Mat. Tech., **112**, 456-464.

[46] Gómez, C., Canales, M., Calvo, S., Rivera, R., Valdés, J. R., and Núñez, J. L. (2011). High and low cycle fatigue life estimation of welding steel under constant amplitude loading: analysis of different multiaxial damage models and in-phase and out-of-phase loading effects. Int. J. of Fatigue, **33**, 578-587.

[47] Chen, X., An, K., and Kim, K. S. (2004). Low-cycle fatigue of 1Cr-18Ni-9Ti stainless steel and related weld metal under axial, torsional and 90° out-of-phase loading. Fatigue Fract. Eng. Mater. Struct., **27**, 439-448.

[48] Han, C., Chen, X., and Kim, K. S. (2002). Evaluation of multiaxial fatigue criteria under

irregular loading. Int. J. of Fatigue, **24**, 913-922.

[49] Chaves, V., Navarro, A., and Madrigal, C. (2015). Stage I crack directions under in-phase axial-torsion fatigue loading for AISI 304l stainless steel. Int. J. of Fatigue, **80**, 10-21.

Fig. 1 Summary of the equivalent damage parameters considered

Authors	Non-proportional loading factor l_{np}	Non-proportional coefficient f_{np}	Damage parameter
Kanazawa [11-12]	$\frac{\gamma_{a,\Delta 45}}{\gamma_{a,max}}$	$1+\alpha_{np} l_{np}$	$\gamma_{eq} = k \cdot \gamma_{max} \cdot f_{np}$
Fatemi[14]	$\frac{\sigma_n^{max}}{\sigma_y}$	$1+\alpha_{np} l_{np}$	$\gamma_{eq} = \frac{\gamma_{max}}{2} \cdot f_{np}$
Itoh[16]	$\frac{1.57}{T\varepsilon_{I max}} \int_0^T \lvert \sin \xi(t) \rvert \varepsilon_I(t) dt$	$1+S\frac{\sigma_b - \sigma_y}{\sigma_b} l_{np}$	$\varepsilon_{eq} = f_{np} \Delta \varepsilon_I$
Borodii [20][22]	$\left(\left\lvert \oint_{L'} \vec{e} \times d\vec{e} \right\rvert / \left\lvert \oint_{L_0} \vec{e} \times d\vec{e} \right\rvert \right)^r$	$(1+k\sin\theta)(1+\alpha_{np} l_{np})$	$\varepsilon_{eq} = f_{np} \Delta \varepsilon_I$
He Guoqiu [23]	$K_c \frac{\left(\bar{S}_n / \bar{S}_p\right)^{-1/2} - 1}{\left(\bar{S}_c / \bar{S}_p\right)^{-1/2} - 1}$	$(1+\alpha_{np} l_{np})^{1/n}$	$\gamma_{eq} = k \cdot \frac{\Delta \gamma_{max}^p}{2} \cdot \left(1+\alpha_{np} f_{np}\right)^{1/n}$
SB Lee[15]	$\sin\phi$	$2(1+\alpha_{np}\sin\phi)$	$\sigma_{eq} = \sigma_a \left[1 + \left(\frac{b_{-1}}{2t_{-1}} \frac{2\tau_a}{\sigma_a} \right)^{f_{np}} \right]^{1/f_{np}}$
Li Jing[24]	/	$1+\frac{\Delta \sigma_n}{2\sigma_{0.2}}$	$\varepsilon_{eq} = \frac{\Delta \gamma_{max}}{2} + f_{np} \frac{\Delta \varepsilon_n}{2}$

Figure 2 Summary of direct damage parameters concerned

Authors	The way to consider non-proportionality effect	Direct damage parameters
Susmel[30]	$\rho = \frac{\sigma_n^{max}}{\tau_a}$	$\tau_{eq} = \tau_a + \left(t_{-1} - \frac{f_{-1}}{2} \right) \rho$
Morel [26]	$H = \frac{T_\Sigma}{C_A}$	$N_f = p \ln\left(\frac{C_A}{C_A - \tau_{-1}} \right) + q \frac{\tau_{-1}}{C_A - \tau_{-1}} - \frac{r}{C_A}$
Spagnoli[28]	The critical plane deflection angle δ	$\sigma_{eq} = \sqrt{\left(\frac{\sigma_{af}}{\tau_{af}} \right)^2 C_a^2 + N_{max}^2}$
Skibicki[36]	$H_s = \frac{\int_\alpha \left(\tau_\alpha^{MDP} \cdot W \right)}{\pi \left(\tau_{\alpha_{CPA}}^{MDP} \right)^2 / 2}$	$\tau_{eq} = \tau_{\alpha_{CPA}}^{MDP} + \left(1 + \frac{t_{-1}}{b_{-1}} H^n \right)$

Figure 3 The mechanical properties of materials

Materials	E/GPa	v	σ_y/MPa	f_{-1}/MPa	t_{-1}/MPa	K′ /MPa	n′
TC4 [42]	116	0.31	930	346	158	854	0.0149
LY12CZ[43]	73	0.30	400	168	120	870	0.0970
SM45C[15]	186	0.28	496	442	311	1246	0.1200
30CrMnSiA [43]	203	0.30	1105	508	293	-	-
1045 [14]	202	0.28	382	303	175	1258	0.2080
C35 [41]	214	0.29	350	240	168	-	-
304 [45]	185	0.30	325	138	83	812	0.1250
S355J2[45]	196	0.30	355	220	165	721	0.1258
1Cr–18Ni–9Ti[47]	193	0.30	310	242	102	1115	0.1304
SNCM630 [48]	196	0.27	951	488	320	1056	0.0540

Figure 4 The fatigue properties of materials

Materials	σ_f' /MPa	ε_f'	b	c	τ_f' /MPa	γ_f'	b_0	c_0
TC4[42]	1117	0.5790	-0.0490	-0.6790	716.9	2.240	-0.0600	-0.8000
LY12CZ[43]	759	0.215	-0.0638	-0.6539	-	-	-	-
SM45C[15]	843	0.3270	-0.1050	-0.5460	559	0.496	-0.1080	-0.4690
30CrMnSiA [43]	1864	2.788	-0.086	-0.7735	-	-	-	-
1045 [14]	930	0.2980	-0.1060	-0.4900	505	0.413	-0.0970	-0.4450
C35 [41]	-	-	-	-	-	-	-	-
304 [45]	1000	0.1710	-0.1140	-0.4020	709	0.413	-0.1210	-0.3530
S355J2[45]	525	0.0662	-0.0521	-0.3987	386	0.081	-0.0503	-0.3317
1Cr–18Ni–9Ti[47]	1124	0.8072	-0.0910	-0.6650	644	0.812	-0.0880	-0.5330
SNCM630 [48]	1272	1.5400	-0.0730	-0.8230	858	1.510	-0.0610	-0.7060

Note: “-” means that fatigue curves are estimated by fitting data points

Figure 5 The experimental data and predicted life of four criterions

Materials	N_{exp}	N_{cal}			
		Susmel	Spagnoli	Kanazawa	Itoh
TC4[41]	6200	35,466	1074	1100	660
	72,141	52,782	1200	468	105,874
	241,250	433,433	29,062	3884	2,585,606
	961,806	732,288	64,284	6527	5,744,415
	67,965	677,053	372,055	10,344	153,159
	111,783	∞	134,234	826	696,059
LY12CZ [43]	482,666	367,353	827,597	7821	4,198,500
	76,451	72,327	168,721	4824	158,000
	23,003	15,237	40,152	3060	16,900
	420,261	271,424	619,640	6810	176,000
	63,584	50,639	117,199	3887	10,600
	275,527	200,597	535,607	5556	1,885,300
	57,004	39,372	94,679	3231	68,700
	231,348	145,750	408,476	4666	48,300
	30,893	30,135	78,778	2630	4600
	15,459	22,353	66,303	2013	46,200
	66,940	102,221	350,838	3525	967,200
	14,296	25,562	49,165	1716	260,300
	4634	6531	9451	1006	16,400

Materials	N_{exp}	N_{cal}			
		Susmel	Spagnoli	Kanazawa	Itoh
	37,789	34,947	71,389	1764	496,100
	6811	10,188	13,744	1030	25,300
SM45C [15]	29,900	17,289	29,306	5128	22,432
	35,700	15,230	34,665	7757	16,181
	50,000	109,096	38,619	14,083	19,193
	73,800	24,846	52,172	8680	21,443
	106,000	209,404	69,438	11,501	28,803
	106,000	34,115	70,369	9014	28,198
	112,000	273,832	91,114	19,923	30,566
	131,000	247,077	84,773	24,716	28,465
	333,000	68,287	211,945	11,501	43,296
	431,000	1,125,272	301,980	50,859	40,111
	1,660,000	∞	∞	36,398	256,900
	1,860,000	∞	∞	27,914	95,221
	104,143	75,355	139,564	26,235	22,,985
	92,309	37,347	63,431	15,173	19,735
30CrMnSiA [43]	104,143	259,356	991,849	9244	356,600
	92,309	205,227	558,015	2780	241,058
	71,822	156,446	236,801	541	180,856
	105,211	205,261	411,122	1453	138,467

Materials	N_{exp}	N_{cal}			
		Susmel	Spagnoli	Kanazawa	Itoh
	455,138	444,684	444,466	5215	4,508,564
	246,224	260,233	260,409	3052	2,641,538
	81,795	81,196	81,458	952	826,293
	197,013	190,564	190,823	2235	1,935,670
1045[14]	6050	6751	8154	40,779	522,761
	1080	680	1163	15,200	131,387
	3500	1366	2410	5762	4711
	1100	509	960	1990	1677
	1800	530	271	1395	1380
	980	334	179	714	696
	2450	180	357	1467	1298
	1090	84	174	530	489
C35[40]	667,233	4,512,206	9,074,537	5,710,027	992,443
	317,000	1,465,229	1,682,389	1,254,531	166,349
	565,000	2,571,267	3,907,288	2,651,225	401,802
	927,362	3,603,232	6,478,058	4,191,315	689,342
	203,000	297,959	3,266,172	1811	31,635
	311,000	724,998	∞	5059	106,173
	553,942	1764075	∞	14,652	371,784
	2,000,000	4,292,371	∞	44,108	1,362,616

Materials	N_{exp}	N_{cal}			
		Susmel	Spagnoli	Kanazawa	Itoh
	2,000,000	2,751,738	∞	25,295	707,572
	147,000	122,455	1,055,631	671	9808
	1,000,000	∞	7,613,893	6	∞
	667,095	1,033,949	47,220	0	851,944
	223,572	466,752	8676	0	180,275
	310,503	694,685	20,241	0	388,610
	128,973	313,605	3719	0	84,995
	102,046	210,707	1594	0	40,698
	987,340	1,538,879	110,170	0	1,901,002
304[44]	3560	533	24	8758	1,2399
	3730	720	35	8758	12,399
	45,000	10,060	980	56,903	110,801
	50,000	13,499	1288	54,044	93,264
	1167	3822	638	7427	1100
	6080	8971	1734	38,796	5295
	10,300	81,040	23,769	94,738	12,699
	30700	129,864	42,031	244,622	33,011
	286,400	314,802	123,853	1,936,770	299,520
	333,100	674,372	317,665	1,936,770	299,520
	4090	1925	861	1422	1790

Materials	N_{exp}	N_{cal}			
		Susmel	Spagnoli	Kanazawa	Itoh
	48,500	14,809	8021	15,155	20,535
	65,340	71,996	45,246	15,591	21,176
	33,900	68,490	42,841	15,155	20,535
	83,400	167,675	114,093	36,930	55,164
	1,100,000	187,624	129,023	271,076	618,716
	824,200	406,428	300,556	265,493	602,235
	53,000	89,263	104,431	72,657	26,100
	52,900	140,095	167,881	72,657	26,100
	440,000	308,301	400,244	607,571	250,793
	356,000	323,033	447,104	607,571	250,793
S355J2 [45]	61,935	350,334	63,589	4,938,723	77,681
	129,464	600,727	143,505	∞	163,940
	232,107	638,511	157,345	∞	256,188
	292,690	1,116,042	365,502	∞	426,990
	587,881	1,576,167	615,421	∞	771,854
	111,588	109,320	105,466	22,012	77,679
	158,584	165,751	160,435	29,713	110,488
	230,215	222,831	216,190	41,239	163,937
	428,183	429,663	419,029	59,157	256,182
	57,647	661	244	46,263	19,692

Materials	N_{exp}	N_{cal}			
		Susmel	Spagnoli	Kanazawa	Itoh
	120,993	1193	412	92,829	29,620
	88,117	1628	542	137,762	36,973
	113,733	3224	3192	61,014	37,857
	219,319	6058	5529	135,601	65,154
	360,616	8444	7402	216,152	88,548
	216,056	12,911	31,337	68,511	54,540
	790,266	25,251	55,700	159,577	102,449
	595,355	35,984	75,648	263,175	147,474
	759,229	52,019	104,224	464,285	221,085
	13,700	410	232	13,117	26,779
	50,203	5168	15,096	39,332	19,876
	44,559	2612	4394	46,575	56,802
	287,166	9382	30,544	73,500	48,650
	153,845	12,789	44,308	103,488	84,113
	47,087	844	556	20,144	83,963
1Cr–18Ni–9Ti [46]	200,000	24,564	187,364	58,600	585,994
	12,410	3417	13,179	13340	133,404
	5500	2108	7520	5601	56,014
	3100	593	1955	3049	30,494
	950	305	1027	574	574

Materials	N_{exp}	N_{cal}			
		Susmel	Spagnoli	Kanazawa	Itoh
	81,376	81,869	2462	24,763	24,762
	12,188	11,094	280	5601	5601
	5283	6970	179	1913	1913
	1500	1086	35	574	574
	376	429	17	237	237
	30,028	7435	61,076	6533	6533
	3648	1142	3262	2479	2479
	646	111	199	1085	10,856
	184	28	52	140	140
SNCM630[47]	369	1067	1036	831	425
	591	384	371	1519	671
	1614	1235	1200	4009	1341
	25,96	1794	1745	9498	2357
	39,58	4830	4711	51,209	6281
	30,529	15,796	15,468	188,0274	48,164
	231,112	433,154	428,775	∞	712,630
	892	960	8560	312	708
	2769	4137	26,111	1078	3393
	9859	6517	36,943	1547	6007
	23,092	10,956	54,923	2335	12,704

Materials	N_{exp}	N_{cal}			
		Susmel	Spagnoli	Kanazawa	Itoh
	48,613	79,376	249,091	4513	53,219
	162,566	196,997	498,598	6299	117,317

Note: ∞ refers to life time larger than 10^7 cycles to failure.

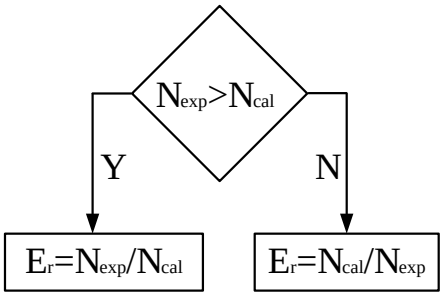

Figure 6 The method to calculate error index E_r

Figure 7 The percentage in different error index E of four criterions

Materials	$E_r \leq 2$				$E_r \leq 3$				$E_r \leq 4$			
	Susmel	Spagnoli	Kanazawa	Itoh	Susmel	Spagnoli	Kanazawa	Itoh	Susmel	Spagnoli	Kanazawa	Itoh
TC4	50%	17%	0%	17%	50%	17%	0%	33%	50%	17%	0%	33%
LY12CZ	100%	53%	0%	20%	100%	80%	0%	40%	100%	87%	0%	53%
SM45C	29%	86%	0%	7%	71%	86%	0%	14%	79%	86%	7%	36%
30CrMnSiA	63%	50%	0%	13%	100%	50%	0%	38%	100%	75%	0%	50%
1045	25%	50%	63%	63%	63%	50%	75%	75%	75%	50%	75%	75%
C35	29%	0%	0%	65%	65%	0%	0%	82%	76%	0%	6%	82%
304	24%	48%	24%	68%	48%	64%	44%	88%	64%	72%	52%	100%
S355J2	16%	36%	44%	52%	24%	36%	52%	64%	28%	44%	60%	80%
1Cr–18Ni–9Ti	36%	43%	57%	57%	43%	50%	79%	79%	64%	64%	93%	93%
SNCM630	85%	46%	0%	92%	100%	62%	38%	92%	100%	77%	46%	92%

Figure 8 The mean value and variance of error index e

Materials	The mean value of E_r				The variance of E_r			
	Susmel	Spagnoli	Kanazawa	Itoh	Susmel	Spagnoli	Kanazawa	Itoh
TC4	18.27	15.97	85.20	6.01	31.99	20.18	63.49	3.38
LY12CZ	1.39	2.39	23.96	6.41	0.21	1.05	19.94	4.98
SM45C	2.96	1.98	15.29	5.64	1.38	1.53	18.19	4.50
30CrMnSiA	1.62	3.36	73.96	6.30	0.61	2.90	34.69	3.88
1045	5.05	3.78	3.83	27.22	4.82	2.56	4.22	45.21
C35	3.14	16.87	3440100	3.29	2.23	14.82	5039386	3.67
304	3.49	15.53	4.26	1.74	2.05	34.70	2.56	0.73
S355J2	24.73	41.31	12.27	2.66	26.41	75.44	21.99	1.60
1Cr–18Ni–9Ti	3.45	13.35	2.12	2.12	2.19	16.25	1.04	1.04
SNCM630	1.63	3.51	14.39	1.48	0.47	2.88	18.18	0.54

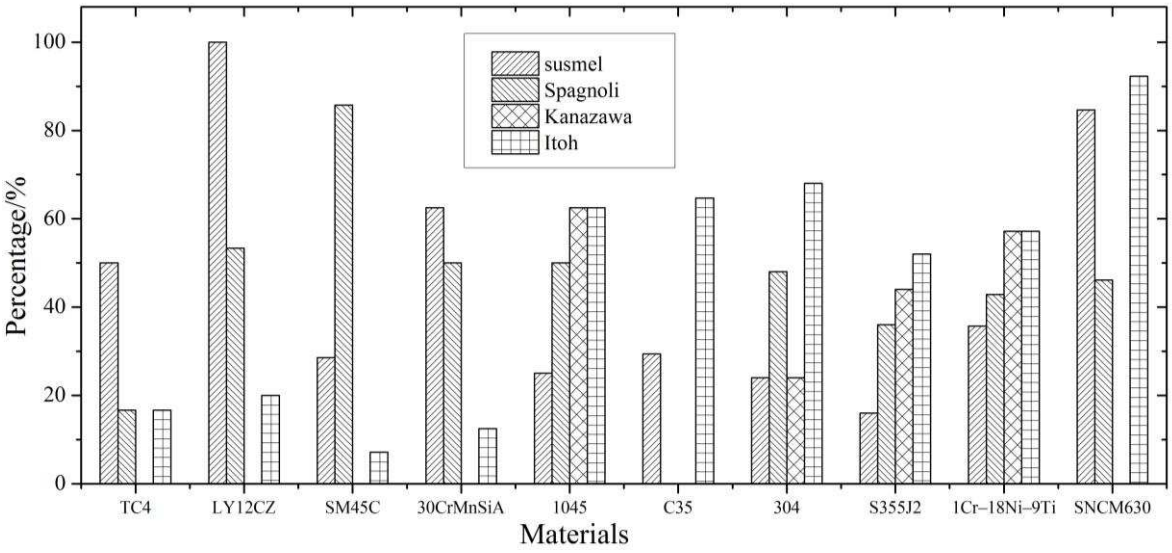

Figure 9 Error index $E_r \leq 2$

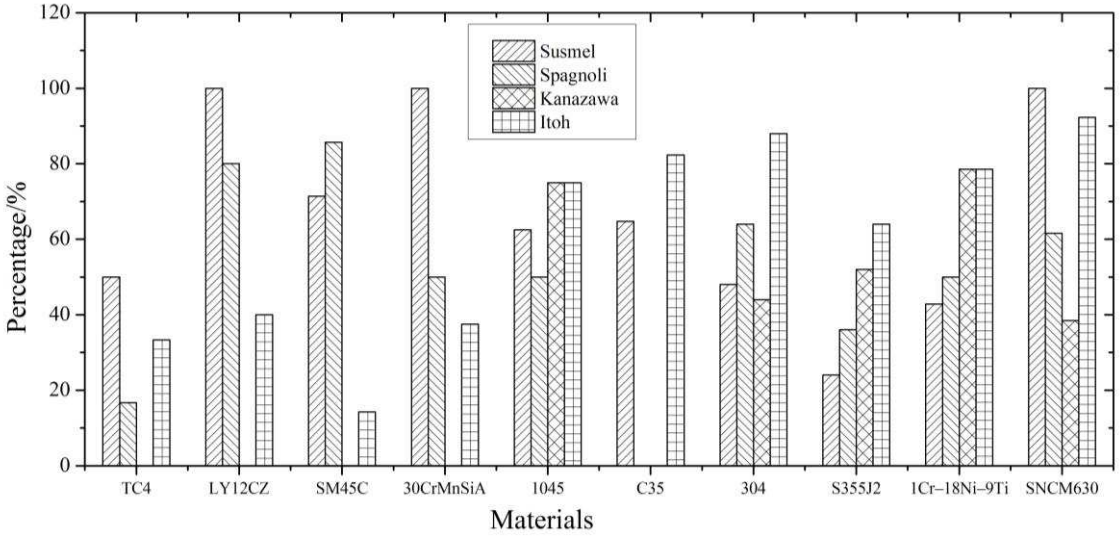

Figure 10 Error index $E_r \leq 3$

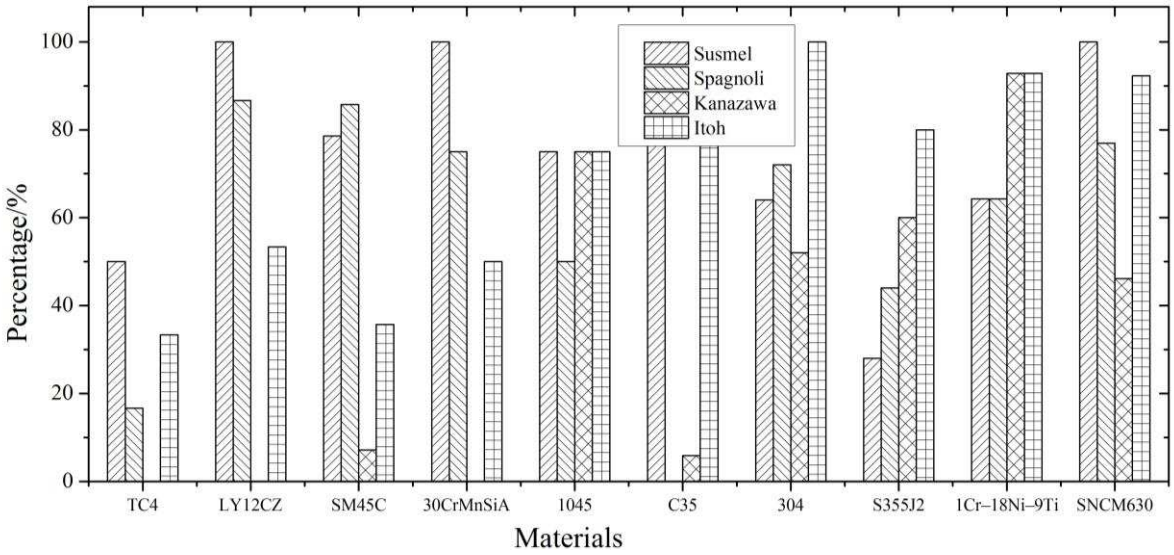

Figure 11 Error index $E_r \leq 4$

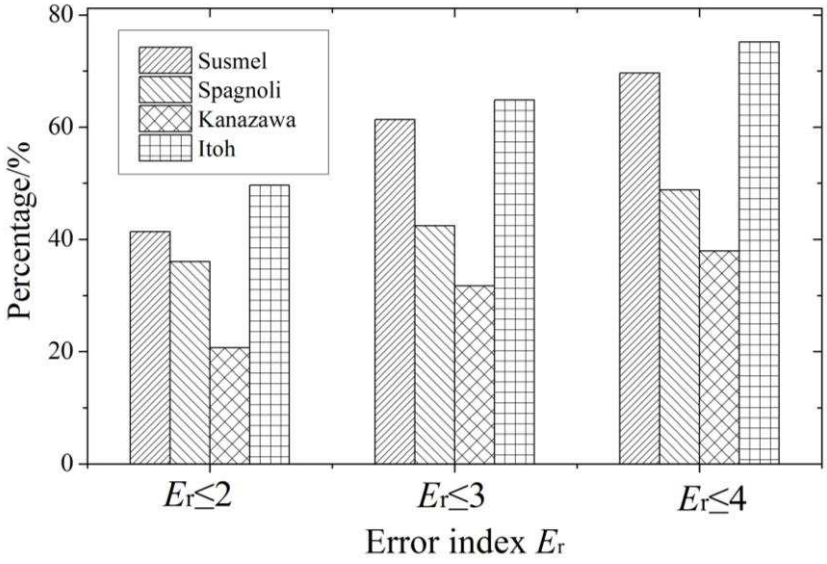

Figure 12 The percentage of 4 kinds of multiaxial fatigue failure criteria

Figure 13 The optimum criterions for these materials

Materials	t_{-1}/f_{-1}	Criterions
1Cr–18Ni–9Ti	0.4234	Kanazawa/Itoh
TC4	0.4570	Susmel
30CrMnSiA	0.5773	Susmel
1045	0.5776	Kanazawa/Itoh
304	0.6029	Itoh
SNCM630	0.6570	Susmel/Itoh
SM45C	0.7036	Spagnoli
C35	0.7042	Itoh
LY12CZ	0.7089	Susmel
S355J2	0.7487	Itoh